Multilevel resistive switching with ionic and metallic filaments

Ming Liu,[1] Z. Abid,[2] Wei Wang,[2,a)] Xiaoli He,[2] Qi Liu,[1] and Weihua Guan[1]
[1]*Laboratory of Nanofabrication and Novel Device Integration, Institute of Microelectronics, Chinese Academy of Sciences, Beijing 100029, People's Republic of China*
[2]*College of Nanoscale Science and Engineering (CNSE), University at Albany, New York 12203, USA*

(Received 30 March 2009; accepted 15 May 2009; published online 9 June 2009)

The resistive random access memory (ReRAM) device with three distinguishable resistance states is fabricated by doping Cu into a portion of the ZrO_2 oxide layer of the $Ti/ZrO_2/n^+$-Si structure. The temperature-dependent measurement results demonstrate that filaments due to ionic trap-controlled space charge limited current conduction and metallic bridge are formed at different voltages. The formation and rupture of these different conducting filamentary paths in parallel are suggested to be responsible for the multilevel switching with the large resistance ratio, which can be used to establish a reliable multilevel ReRAM solution with variation tolerance. © *2009 American Institute of Physics*. [DOI: 10.1063/1.3151822]

Hysteretic resistive switching has been observed in a variety of materials, including ferromagnetic material such as $Pr_{1-x}Ca_xMnO_3$(PCMO),[1] doped perovskite oxides such as $SrZrO_3$ (Ref. 2) and $SrTiO_3$,[3] organic materials,[4] and binary metal oxides such as NiO,[5] TiO_2,[6] ZrO_2,[7] Cu_xO,[8] ZnO_2,[9] HfO_2,[10] AlO_x,[11] and even amorphous Si (Ref. 12) and doped SiO_2.[13] These materials can establish resistive random access memory (ReRAM) with high density and low-voltage/low-power operations. Recently, HfO_2 and ZrO_2 have attracted extensive attention for ReRAM applications by providing easy fabrication process and full compatibility with the complementary metal-oxide-semiconductor technology.[7,10,14–16] ReRAM devices with these materials can form filaments with different switching properties by changing doping materials and fabrication processes.[14–16] Particularly, when a ZrO_2 sandwiched junction device is programmed, a filament with ionic trap-controlled space charge limited current conduction (SCLC) can be formed in the undoped ZrO_2 layer,[14] while a metallic conduction filament (or metal bridge) can be formed in the Cu-doped ZrO_2 layer.[16] Therefore, the multilevel resistance states can be obtained by forming different filaments inside the device to increase the data storage capability of the device and establish efficient memory circuits.

In this letter, an ultrathin Cu film is introduced into a portion of the ZrO_2 layer of the $Ti/ZrO_2/n^+$-Si device to obtain three resistance levels. The temperature-dependent measurement is carried out to analyze different switching mechanisms for these resistance levels. Compared with the multilevel ReRAM devices based on one switching behavior,[17,18] the proposed device can utilize the properties of different filaments to obtain distinguishable resistance levels with large resistance ratios.

A 70-nm-thick ZrO_2 layer is deposited on a n^+ silicon wafer by the rf sputtering method. Then, a photolithography is performed to pattern horizontal 3-μm-wide stripes, followed by a sputtering process of an about 7-nm-thick Cu ultrathin film. After the first lift-off process, annealing is performed at 600 °C for 30 s to activate Cu atoms in the ZrO_2 layer, and then the top Ti electrode (100-nm-thick) is deposited. Finally, the second lift-off process is used to get the square Ti electrodes (6×6 μm^2), each covering both an undoped stripe (left) and a Cu stripe (right) as shown in Fig. 1.

In order to verify the different doping materials in the left and right sides of the device, we use Auger electron spectroscopy (PHY 660) technique to get the depth profiles. Figure 1 demonstrates that at the Cu-doped region (the right side of the device), the insulator layer consists of ZrO_2 and Cu doping. The 7-nm-thick Cu doping can diffuse and the Cu depth profile is more than 7 nm. The undoped region (the left side of the device) shows a minimum Cu depth.

The (I-V) characteristics of the 6×6 μm^2 device are obtained by using Keithley 4400 Semiconductor Characterization System, exhibiting the reproducible multilevel switching without the requirement of electroforming. As shown in Fig. 2(a), by sweeping the voltage: 0 V→+3 V→0 V→−3 V→0 V (current compliance is 1 mA), the sample shows the bipolar switching with two distinguishable values: R_{off}(~MΩ) and $R_{on\ 1}$(~10 kΩ). As seen in Fig. 2(b), when the voltage is swept from 0 to +5 V and the current compliance is 10 mA, three distinguished states

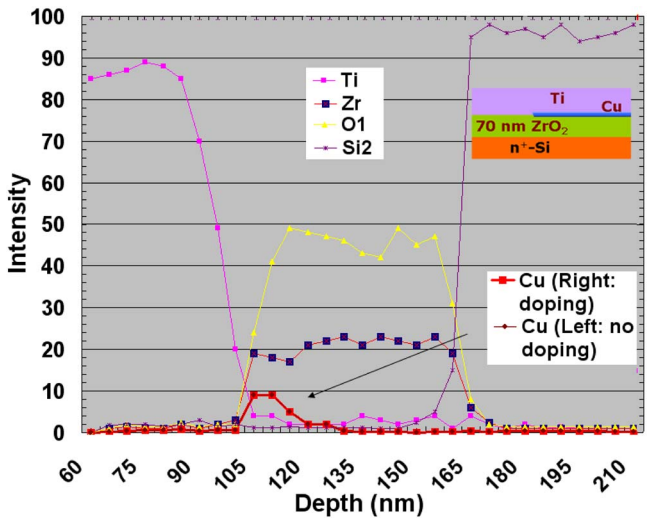

FIG. 1. (Color online) Auger electron spectroscopy result for the undoped (left) and Cu-doped (right) regions.

a)Author to whom correspondence should be addressed. Electronic mail: wwang@uamail.albany.edu. Tel.: 1-518-9567057. FAX: 1-518-4378063.

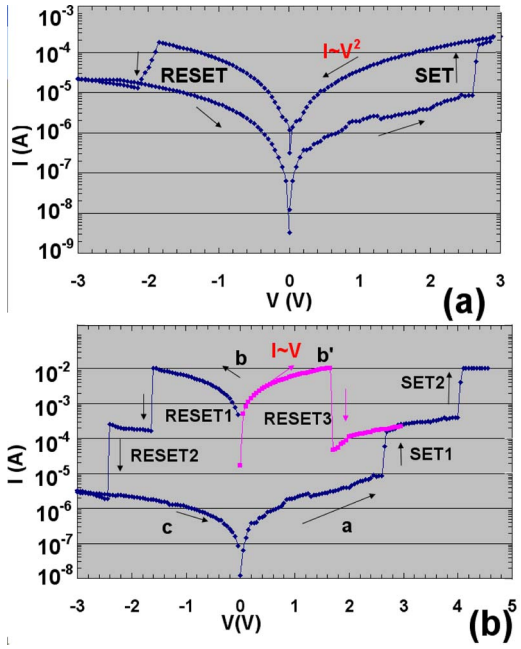

FIG. 2. (Color online) (a) *I-V* curve of the proposed device (from −3 to +3 V) showing two levels. (b) *I-V* curve of the proposed device (from −3 to +5 V) showing three levels: R_{off}, $R_{on\ 1}$, and $R_{on\ 2}$. The positive applied voltages can set the device into $R_{on\ 1}$ and $R_{on\ 2}$, while the negative applied voltages can reset $R_{on\ 2}$ back to $R_{on\ 1}$ and R_{off}. The red curve shows the unipolar reset from $R_{on\ 2}$ to $R_{on\ 1}$. Note: based on (a) and (b), the read voltage of 0.5—1 V can read the three states of the multilevel device.

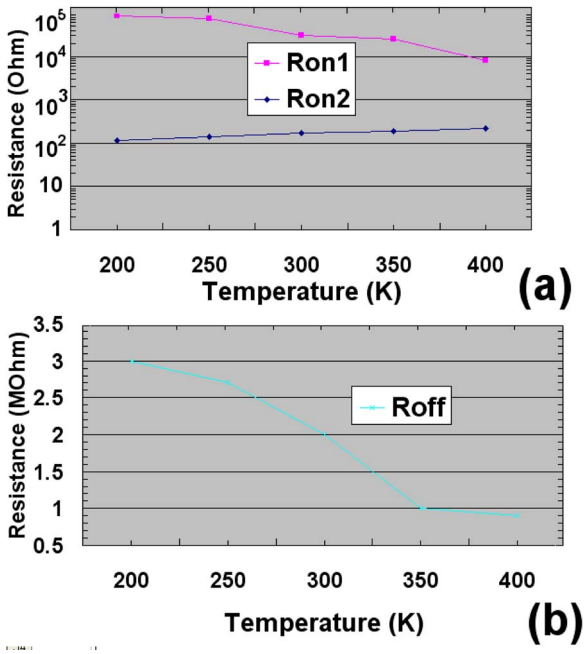

FIG. 3. (Color online) (a) $R_{on\ 1}$ and $R_{on\ 2}$ values according to temperature, (b) R_{off} values according to temperature.

are demonstrated: $R_{off}(\sim M\Omega)$, $R_{on\ 1}(\sim 10\ k\Omega)$, and $R_{on\ 2}(\sim 200\ \Omega)$. It is important to note that the reset process of $R_{on\ 2}$ to $R_{on\ 1}$ shows the nonpolar switching behavior. When $R_{on\ 2}$ is obtained at +4 V, it can be reset to $R_{on\ 1}$ in both positive (~+1.8 V) and negative voltages (~−1.7 V), showing no polarity. However, since the switching from $R_{on\ 1}$ to R_{off} is bipolar [Fig. 2(a)], the switching from $R_{on\ 1}$ back to R_{off} only occurs in the negative region, as shown in Fig. 2(b). We can then use "a-b-c" sweeping to "program" all the three levels and then "erase" them. The read voltages 0.5–1 V can be used to get these resistance levels.

In order to study the device switching mechanisms, we obtained the temperature-dependent resistance values of the device after the SET1 operation ($V_{set\ 1}<3$ V for $R_{on\ 1}$), and after SET2 operation ($V_{set\ 2}>3$ V for $R_{on\ 2}$), respectively. Fig. 3(a) illustrates the $R_{on\ 1}$ and $R_{on\ 2}$ (the read voltage is 0.5 V) as a function of the temperature in the range of 200–400 K. Note that $R_{on\ 1}$ decreases as the temperature increases, demonstrating the ionic filament is formed after the SET1 operation.[16] Such an ionic filament is generally based on the oxygen vacancies in the oxide, showing a combination of Ohmic and square-law conductions.[15,19] As shown in Fig. 2(a), the *I-V* curve of $R_{on\ 1}$ contains a region known as the child's square law region ($I\sim V^2$). It is also noted that after the SET1 process, when the voltage sweeps from +3 V→0 V, the device will maintain the low resistance $R_{on\ 1}$ at the 0 V. Whereas, if the voltage sweeps from −3 V→0 V after the SET1 process, the device will reset and a high resistance value is obtained at 0 V. That is, the reset process can only occur in the negative region. Even though the *I-V* curve is changing in the counterclockwise direction [Fig. 2(a)], the resistance change or variation of the proposed device between ±3V follows the clockwise direction (similar to Figs. 4 and 5 in Ref. 19), reflecting the asymmetric ionic trap-controlled space charge limited current conduction.[19] The electron traps at the top or bottom electrodes can absorb injected electrons.[19] After the traps are filled, the voltage square-law conductance may occur. Since the top and bottom electrodes of the proposed device are based on different materials with different trap potentials, the trap structures of the SCLC filament are asymmetric. It was demonstrated in Ref. 19 that for the high-barrier top electrode and low-barrier bottom electrode case, the SCLC filament will exhibit the clockwise resistance change, which might be used to explain the ionic filament switching behavior of the proposed device.

The temperature-dependent measurement also illustrates that $R_{on\ 2}$ is increasing linearly with the temperature, demonstrating that a metallic filament is formed after the SET2 operation.[16] The metal ions such as Cu or Ag can diffuse into the oxide to form the metallic filament,[10,16] which was directly observed in the recent transmission electron microscopy (TEM) images and also with the high-resolution energy dispersive X-ray spectroscopy (EDX) analysis.[20] The set and reset voltages of the metallic switching can be higher than those of the ionic switching, since the formation of the metallic filament might require a higher electric field or voltage than the ionic SCLC filament.[15,16] During the reset process, the rupture of the metallic filament is generally due to local heating[10,16,21–23] with no polarity, which is consistent with the nonpolar RESET1 or RESET3 operations in Fig. 2(b).

It is noteworthy that the above analysis of the ionic and metallic filaments is based on the temperature-dependent electrical measurement results. The direct TEM measurement will be carried out in our future work to verify the different switching mechanisms of the proposed device.

For the purpose of comparison, we made two devices ($6\times 6\ \mu m^2$) with either a complete layer of Cu doping or without Cu doping using the same sputtering and photolithography methods. The resistance of the device without Cu

doping is around 20 kΩ and the one with Cu doping is in the range of 100–200 Ω, which suggests that the switching mechanism of the three-level device might be the formation and rupture of the ionic and metallic bridge filaments connected in parallel.

For the set processes, after SET1 operation, $R_{on\ 1}$ is obtained. The current density is governed by the equation:[24] $J=9\varepsilon_r\varepsilon_0\mu V^2/8L^3=V/R_{on1}A$, where ε_o is the permittivity of free space, ε_r is the dielectric constant of the ZrO_2 oxide, μ is the mobility of the conducting electrons in the ionic filament of ZrO_2, L is the conducting filament length in the oxide, V is the read voltage (0.5–1 V), and A is the effective area of the SCLC filament. $R_{on\ 1}$ can then be calculated in the range of 20–40 kΩ, which is in close agreement with the measured result for the read voltage between 0.5 and 1V.

After the SET2 operation, $R_{on\ 2}$ is around 200 Ω and its current has a linear relationship with the applied voltage. Thus, we suggest that this resistance is mainly due to that of the metal bridge filament:$R=h/2e^2N$, where h is Planck's constant, e is electron charge, and N represents the number of conducting channels in the filament.[16,22] Thus, R can be calculated to be around 300 Ω. The equivalent resistance of this metallic filament and the ionic SCLC filament connected in parallel can represent $R_{on\ 2}$, which is consistent with the measurement result about 200 Ω.

For the reset processes, the metallic filament shows the nonpolar switching property that can be explained by the local heating and the thermal dissolution of the filament.[22,23] This filament can be turned off when a low voltage and a high current are applied regardless of the polarity.[16] Therefore, $R_{on\ 2}$ can be reset to $R_{on\ 1}$ in both negative and positive regions. Then, the ionic bipolar SCLC filament can be reset using a high voltage and a strong electric field in the negative voltage region.[15]

The significance of this study is to demonstrate the proposed device can utilize different filaments to achieve the multilevel ReRAM switching with a large resistance ratio. Since the filaments and switching behaviors are different for $R_{on\ 1}$ and $R_{on\ 2}$, the $R_{on\ 1}/R_{on\ 2}$ ratio is greater than 10. Note that the $R_{on\ 1}/R_{off}$ ratio is also much greater than 10. Thus, even when the variations of three resistance values are around ten times (a number of testing results demonstrated such variations[9,14–16]), we can still have three distinguishable states. The multiple states with such variation tolerance might not be easily obtained in the device with a single type of filament.[17,18] Therefore, the proposed device is a promising solution to establish reliable multilevel memory systems and is expected to have a significant impact to the integrated circuit industry.

The endurance characteristic of the three-level device is obtained at room temperature. During more than 100 cycles of "SET1-Read-SET2-Read-RESET1-Read-RESET2-Read," the three-level switching property still exists and the variations of the resistances are around seven times. The retention is also verified and the three resistance values are stable for over 2000 s. During the experiments, we made 40 samples of the proposed devices using the 600 °C annealing process and 40 samples using the 400 °C annealing temperature. In the first group of samples, 18 devices exhibit the hysteresis resistances. However, only four devices have the reproducible three-level switching and 14 samples show the two-level nonpolar switching behavior. The temperature-dependent measurement results show that the filaments formed in these 14 samples are metallic. In the second group of samples, nine devices show two-level switching and seven devices show three-level switching. Thus, it is suggested that if the Cu doping has a large diffusion due to a high annealing temperature inside the device, the SCLC filament might not be observed. The three-level devices might require a limited Cu diffusion and a low annealing temperature.

In conclusion, we have introduced an approach to build multilevel ReRAM devices by partially doping Cu into the ZrO_2 layer to obtain different filaments and switching behaviors in one device. It is similar to building one ionic device and one metallic device in parallel but in a more compact form. Since the resistance levels are due to different filaments, distinguishable levels with large resistance ratios can be obtained, leading to variation tolerance. This approach can also be extended to other materials to build a variety of ReRAM multilevel devices for future memory applications.

This work is partially supported by NSF (Grant No. 0829824), SRC FRCP, NSFC (Grant No 60825403), and 973 project (Grant Nos. 2006CB302706, 2006CB806204).

[1] A. Sawa, T. Fujii, M. Kawasaki, and Y. Tokura, Appl. Phys. Lett. **85**, 4073 (2004).
[2] C.-C. Lin, B.-C. Tu, C.-C. Lin, C.-H. Lin, and T.-Y. Tseng, IEEE Electron Device Lett. **27**, 725 (2006).
[3] T. Fujii, M. Kawasaki, A. Sawa, H. Akoh, Y. Kawazoe, and Y. Tokura, Appl. Phys. Lett. **86**, 012107 (2005).
[4] Y. Song, Q. D. Ling, S. L. Lim, E. Y. H. Teo, Y. P. Tan, L. Li, E. T. Kang, D. S. H. Chan, and C. Zhu, IEEE Electron Device Lett. **28**, 107 (2007).
[5] J.-W. Park, J.-W. Park, K. Jung, M. K. Yang, and J.-K. Lee, J. Vac. Sci. Technol. A **24**, 2205 (2006).
[6] B. J. Choi, D. S. Jeong, S. K. Kim, C. Rohde, S. Choi, J. H. Oh, H. J. Kim, C. S. Hwang, K. Szot, R. Waser, B. Reichenberg, and S. Tiedke, J. Appl. Phys. **98**, 033715 (2005).
[7] Y. Lee, S. Bae, and S. J. Fonash, IEEE Electron Device Lett. **26**, 900 (2005).
[8] A. Chen, S. Haddad, Y. C. Wu, Z. Lan, T. N. Fang, and S. Kaza, Appl. Phys. Lett. **91**, 123517 (2007).
[9] N. Xu, L. Liu, X. Sun, X. Liu, D. Han, Y. Wang, R. Han, J. Kang, and B. Yu, Appl. Phys. Lett. **92**, 232112 (2008).
[10] W. Guan, S. Long, Q. Liu, M. Liu, and W. Wang, IEEE Electron Device Lett. **29**, 434 (2008).
[11] K. M. Kim, B. J. Choi, B. W. Koo, S. Choi, D. S. Jeong, and C. S. Hwang, Electrochem. Solid-State Lett. **9**, G343 (2006).
[12] C. Schindler, S. C. P. Thermadam, R. Waser, and M. N. Kozicki, IEEE Trans. Electron Devices **54**, 2762 (2007).
[13] S. H. Jo and W. Lu, Nano Lett. **8**, 392 (2008).
[14] Q. Liu, W. Guan, S. Long, M. Liu, S. Zhang, Q. Wang, and J. Chen, J. Appl. Phys. **104**, 114514 (2008).
[15] Q. Liu, W. Guan, S. Long, R. Jia, M. Liu, and J. Chen, Appl. Phys. Lett. **92**, 012117 (2008).
[16] W. Guan, M. Liu, S. Long, Q. Liu, and W. Wang, Appl. Phys. Lett. **93**, 223506 (2008).
[17] S. H. Jo, K.-H. Kim, and W. Lu, Nano Lett. **9**, 496 (2009).
[18] J. J. Yang, M. D. Pickett, X. Li, D. A. A. Ohlberg, D. R. Stewart, and R. S. Williams, Nat. Nanotechnol. **3**, 429 (2008).
[19] Y. Xia, W. He, L. Chen, X. Meng, and Z. Liu, Appl. Phys. Lett. **90**, 022907 (2007).
[20] Y. C. Yang, F. Pan, Q. Liu, M. Liu, and F. Zeng, Nano Lett. **9**, 1636 (2009).
[21] Y. Zhou, S. Sreekala, P. M. Ajayan, and S. K. Nayak, J. Phys.: Condens. Matter **20**, 095209 (2008).
[22] U. Russo, D. Ielmini, C. Cagli, A. L. Lacaita, S. Spiga, C. Wiemer, M. Perego, and M. Fanciulli, Tech. Dig. - Int. Electron Devices Meet. **2007**, 775.
[23] C. Schindler, S. C. P. Thermadam, R. Waser, and M. N. Kozicki, IEEE Trans. Electron Devices **54**, 2762 (2007).
[24] M. A. Lampert and P. Mark, *Current Injection in Solids* (Academic, New York, 1970).